

CHAPTER-V

C H A P T E R - V  
-----

THE PROPERTIES OF n-Bi<sub>2</sub>S<sub>3</sub> BASED PHOTOELECTROCHEMICAL  
-----  
(PEC) CELLS.  
-----

5.1 Introduction. -----	126
5.2 Experimental Details. -----	127
5.3 Results and Discussion. -----	128
5.3.1 Electrical properties.	129
a) Current-voltage characteristic in dark.	
b) Capacitance-voltage characteristic in dark.	
c) Current-voltage characteristic in light.	
5.3.2 Optical properties. -----	141
a) Photoresponse.	
b) Spectral response.	
c) Speed of response.	

## 5.1 Introduction .

-----  
In recent years, semiconducting chalcogenide thin films have found worldwide applications in various fields of science and technology including solar cells. Solar cells are considered to be one of the possible answers to the depleting resources of fossil fuels. The prohibitive cost of single crystal solar cells has turned the interest of scientific community to the possibility of using semiconductor thin films which are prepared by either a chemical or by a physical methods. Complicated instrumentation, wastage of material, high cost per surface area of deposition, and instability of some compounds at the deposition temperature are a few of the many disadvantages of physical methods. On the other hand, simple, ease of preparation, less quantity of active materials, low cost per surface area of deposition and doping capabilities are distinct advantages of chemical methods. The semiconductors which possess appropriate band gap are effective in solar energy conversion. In this respect, bismuth sulphide seems to be a promising material, since it is a direct band gap ( $E_g \approx 1.4 \text{ eV}$ ), material and shows a strong absorption of light of wavelengths shorter than 900 nm. Solar cells can be made by the solid state junctions and also by the semiconductor - liquid junctions (PEC's), the later has certain potential advantages : such as junction formation by merely immersing the electrode in a suitable

electrolyte, minimization of lattice mismatch and thermal expansion problems, and wide choice and control over the redox potentials in solution.

Since the photovoltaic properties are directly related to the material properties, choice lies both for the preparation method and characterisation techniques. Only a few methods have been used to prepare and characterise the bismuth trisulphide in single crystal and polycrystalline forms and its different aspects of electrochemical behaviour are reported [ 16, 18, 26, 40, 44, 92, 98, 103, 109 ]. The optical to electrical conversion efficiency so far reported is quite below the expectation and is generally supposed to be due to its poor conductivity [ 16, 18, 26 ]. Taking in to account the above facts, we have deposited bismuth trisulphide thin films by a chemical deposition process and are utilised to form a semiconductor - liquid junction. Section 5.2 gives the necessary experimental details. In section 5.3, the experimental observations on dark I-V and C-V characterisations, power output curve, barrier height determination, photo, spectral, and speed of responses have been discussed.

## 5.2 Experimental Details

-----

Thin film photoelectrodes of bismuth trisulphide have been prepared by a chemical deposition process as described in section 3.3. While depositing the samples the preparative

conditions were selected as mentioned in the section 4.3.1. Electrochemical photovoltaic cell was fabricated by employing thin film  $\text{Bi}_2\text{S}_3$  sample as a photoelectrode, an equimolar composition of 1M NaOH - 1M  $\text{Na}_2\text{S}$  - 1M S as an electrolyte and a CoS treated graphite rod as a counter electrode. The cell has been characterised for its I-V and C-V characteristics in dark, I-V characteristic in light (power output) as discussed in section 3.5.2 (i). The barrier height in dark was determined by noting the reverse saturation current of a cell for a constant applied voltage at different temperatures. The optical properties such as photoresponse, spectral response and speed of response have been studied as outlined in 3.5.2 (ii). The photoelectrochemical cell performance has been studied in terms of its various parameters and the results are explained on the basis of electrical and optical properties of the thin films.

### 5.3 Results and Discussion.

-----  
The results reported by earlier workers shows that, the exposure of n -  $\text{Bi}_2\text{S}_3$  photoelectrode to an electrolyte solution dramatically decreases the performance of a cell. This coupled with some other experimental facts made us clear that the method of preparation of the material will not yield satisfactory results in a reproducible fashion. Apparently crystallites of certain minimum dimensions are necessary for the preparation of photoactive electrodes of n- $\text{Bi}_2\text{S}_3$ . X-ray diffraction and optical microscopy have shown that the

films of  $\text{Bi}_2\text{S}_3$  prepared by various deposition methods consist of small crystallites which are not sufficient to absorb all the incident photons. Thus it is proper that the grain size should be large enough compared with the optical absorption depth  $\{ 110 \}$ . Therefore, in this work we have used polycrystalline  $\text{Bi}_2\text{S}_3$  thin film as one of the active electrodes to form a photoelectrochemical cell. The nature of contact between the  $\text{Bi}_2\text{S}_3$  thin film and the stainless steel was tested and the analysis of equilibrium I-V characteristic yields a contact resistance of 40 ohms. Silver paint was utilised for drawing the ohmic contacts as it provides good ohmic contacts to n- $\text{Bi}_2\text{S}_3$   $\{ 16 \}$ .

### 5.3.1 Electrical Properties :

The electrical properties, namely, a) Current - Voltage characteristic in dark, b) Capacitance-Voltage characteristic in in dark , c) Current-Voltage characteristic in light are studied.

#### a) Current - Voltage characteristic in dark :

The current-voltage characteristic in dark of a PEC cell consisting of  $\text{Bi}_2\text{S}_3$  active electrode is shown in fig.5.1. It is seen that the voltage called as the dark voltage,  $V_D$ , and current called as the dark current,  $I_D$ , are generated in a cell. Polarity of the dark voltage is negative towards  $\text{Bi}_2\text{S}_3$  and positive towards the counter electrode. The dark voltage originates from the difference between two half cell

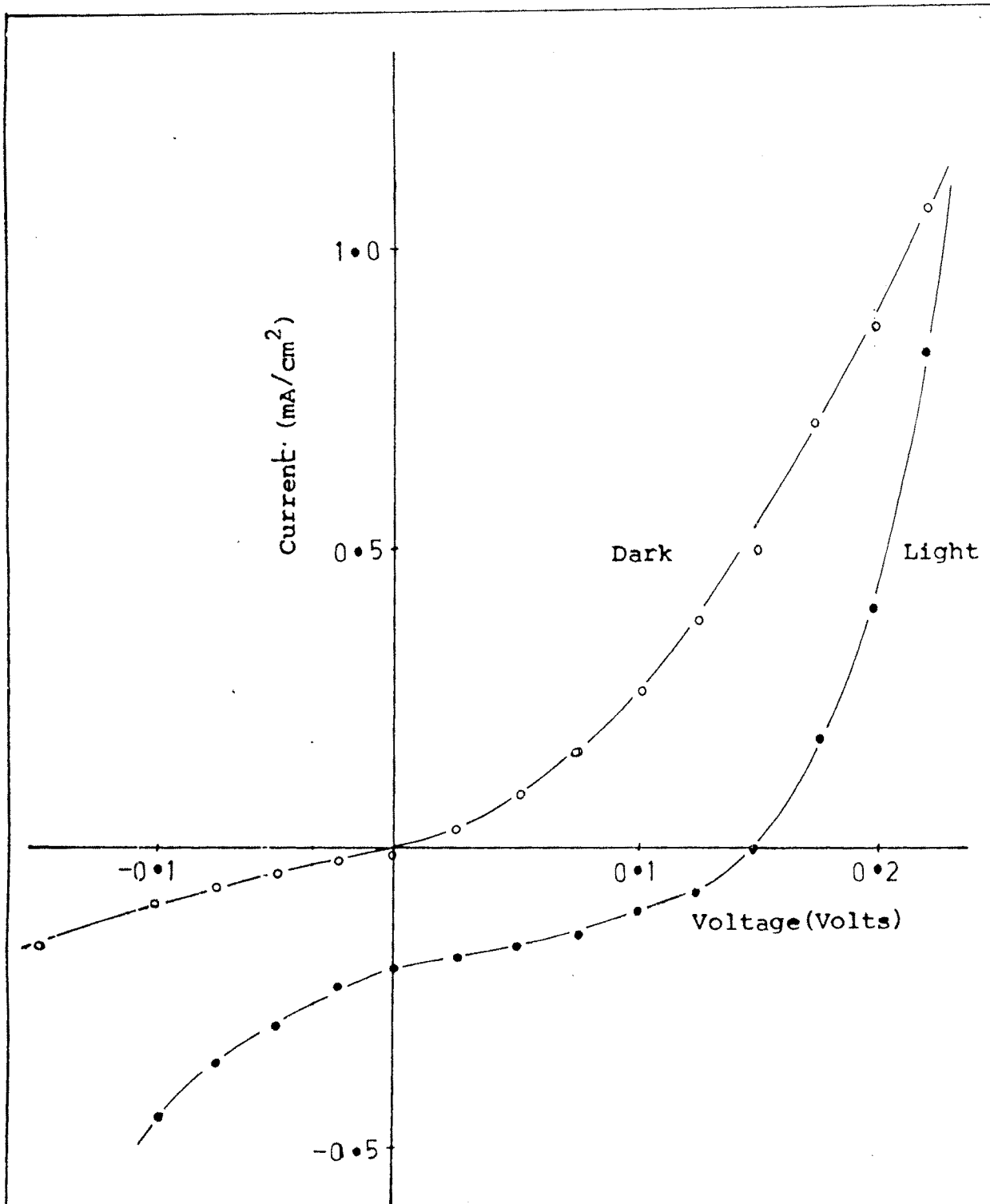


Fig.5.1. Current-Voltage characteristics in:

- I) ○-dark, and
- II) ●- light.

potentials in a PEC cell and can be written as [111]:

$$E = E_{n-Bi_2S_3} - E_{carbon} \quad \dots 5.1$$

where  $E_{n-Bi_2S_3}$  and  $E_{carbon}$  are the half cell potentials developed when  $Bi_2S_3$  photoelectrode and carbon counter electrode are dipped into an electrolyte. From the observed polarity of the voltage it is seen that,

$$E_{n-Bi_2S_3} < E_{carbon} \quad \dots 5.2$$

The existence of a dark current,  $I_D$ , in a cell suggests that there is some deterioration of the active photoelectrode material in dark. In order to understand the charge transfer process across the semiconductor electrolyte interface, the dynamic I-V curve shown in fig.5.1 is further analysed. It is seen that forward current increases rapidly with the bias voltage. The increase of forward current can be ascribed to a small contact barrier height and increase in tunneling mechanism [112,113]. The current in reverse bias condition does not saturate but increases with an applied voltage. Following are possible reasons [112]: i) The effective barrier height ( $\Phi_B$ ) decreases, because of the interfacial layer, ii) Electron - hole pairs are thermally generated in the depletion region of the semiconductor under high reverse bias condition, and iii) The current increases due to the onset of an electron injection from the electrolyte because the barrier becomes thin enough for tunneling to take place. The nature of the I-V curve of a cell can be explained on the

basis of the nature of the charge transfer process given by the Butler - Volmer relation as [59].

$$I = I_0 \left[ \exp. \left( (1-\beta) \frac{V \cdot F}{RT} \right) - \exp. \left( - \beta \frac{V \cdot F}{RT} \right) \right] \quad \dots 5.3$$

where,  $I_0$  is equilibrium exchange current density,  $\beta$  is the symmetry factor,  $V$  is the over voltage,  $R$  is the universal gas constant and  $F$  is the Faraday constant,  $T$  is the absolute temperature.

When  $\beta = 0.5$  equation (5.3) becomes :

$$I = I_0 \left[ \exp. \left( \frac{V \cdot F}{2RT} \right) - \exp. \left( - \frac{V \cdot F}{2RT} \right) \right] \quad \dots 5.4$$

and is further expressed as :

$$I = 2 I_0 \cdot \sinh \left( \frac{F \cdot V}{2RT} \right) \quad \dots 5.5$$

The  $I$  vs.  $\sinh V$  curve is symmetrical. A symmetry factor of 0.5 corresponding to a symmetrical barrier yields a symmetrical  $I$  vs.  $V$  curves. This means that interface cannot rectify a periodically varying potential and /or current.

If  $\beta \neq 0.5$  then  $I$  vs.  $V$  curve would not be symmetrical and the interface has rectifying properties called as Faradaic rectification [59]. The nonsymmetrical nature of the  $I$ - $V$  curve in the forward and reverse bias configuration observed in fig.5.1 shows that the junction formed in the PEC cells are rectifying and analogous to a Schottky barrier junction. The value of junction qualify factor in dark ( $n_d$ ) is determined from the variation of  $\log.I$  vs.  $V$  in response to Schottky diode equation for the

semiconductor electrolyte interface. The variation of  $\log I$  vs.  $V$  is straight line and is shown in fig 5.2. The magnitude of  $n_d$  can be determined from high voltage region of this plot. The value of  $n_d$  is found to be 3.22. It is seen further that the value of dark quality factor is greater than one indicating that the junctions are non-ideal. The higher value of  $n_d$  revealed that the dark I-V characteristics are often influenced by recombination mechanism and series resistance effects [41, 114].

The barrier height (built in potential) of a cell is determined by measuring the reverse saturation current as a function of temperature at a fixed applied voltage. For schottky barrier junction, the reverse saturation current ( $I_0$ ) is related to the built in potential ( $\Phi_B$ ) [115, 116]:

$$I = A T^2 \exp. (-\Phi_B / KT) \quad \dots 5.6$$

where,  $A$  is Richardson's constant and  $\Phi_B$  is the barrier height at equilibrium. The energy level diagram for both semiconductor-metal and semiconductor - electrolyte junctions are identical to each other and hence equation of S-M junction have been applied to S-E junction by many workers [115, 116].

The reverse saturation current is observed to vary exponentially with temperature. The variation of  $\log (I_0/T^2)$  vs.  $1/T$  is displayed in fig 5.3 The slope of this plot gives built-in potential ( $\Phi_B$ ).

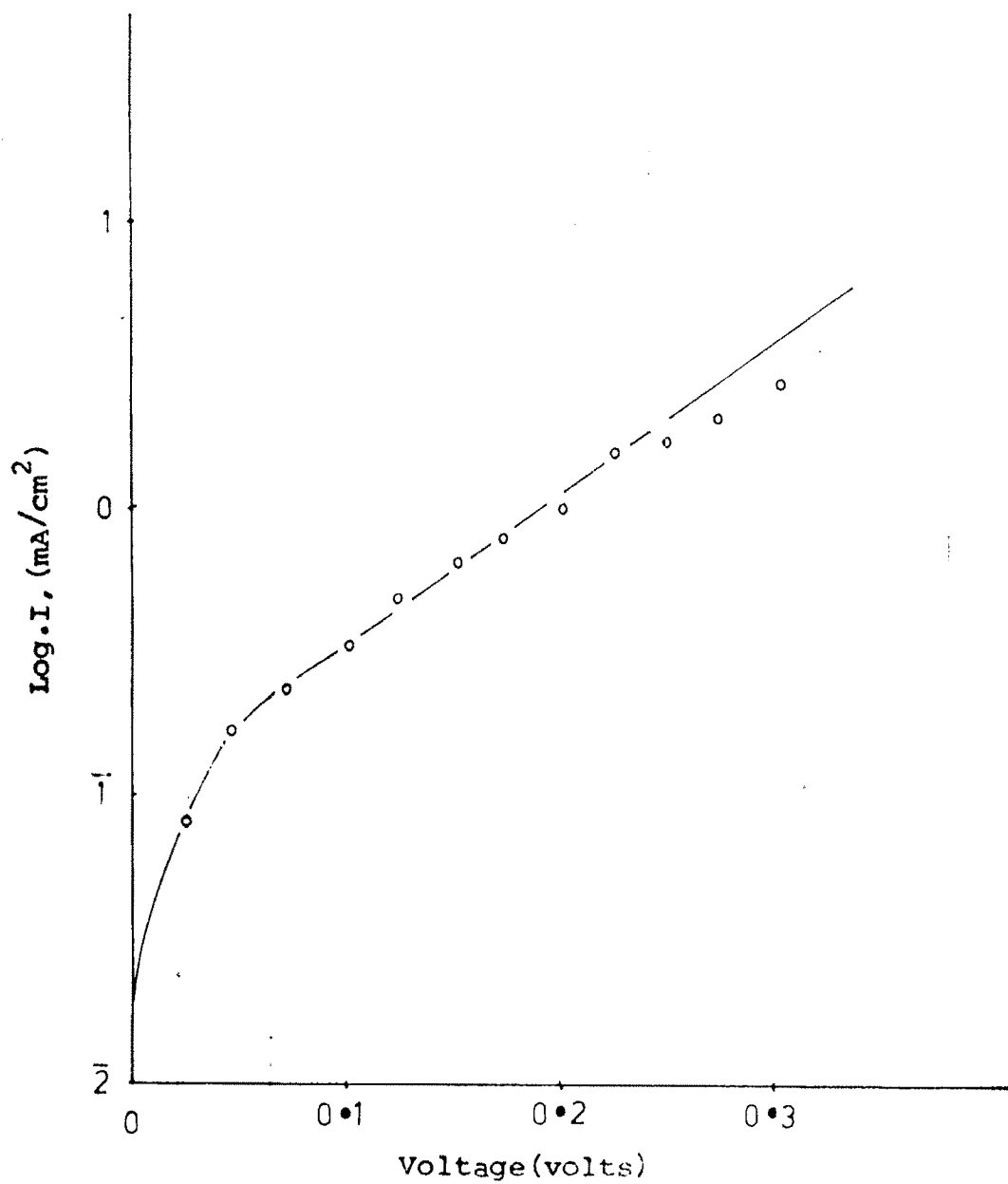


Fig.5.2. Variation of  $\log \cdot I$  vs.  $V$  for a Cell formed with  $n\text{-Bi}_2\text{S}_3$  Photoelectrode.

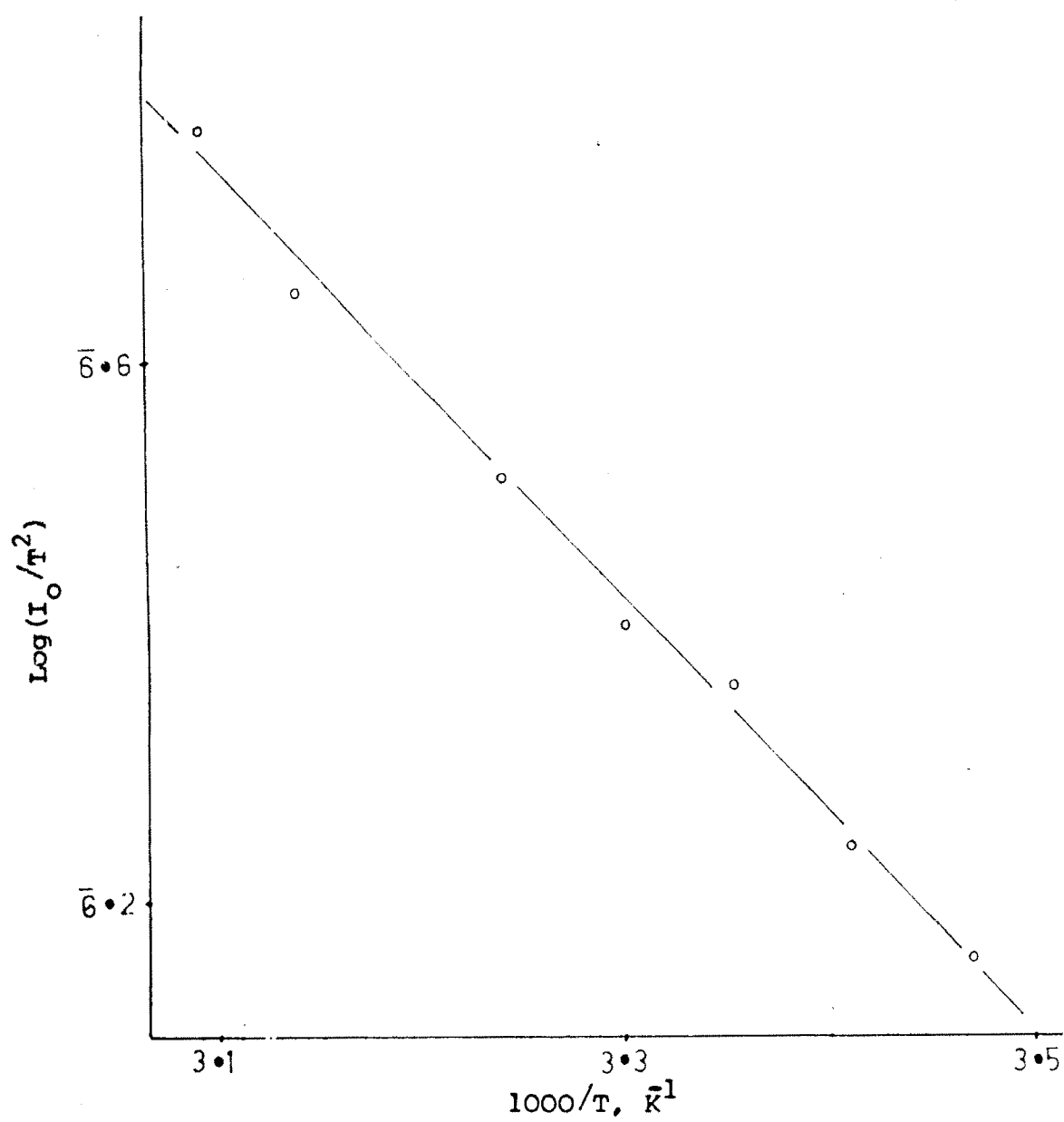


Fig.5.3. Determination of barrier height,  $\bar{\phi}_B$  .

b) Capacitance -Voltage characteristic in dark :

The electrode / electrolyte interface can further be analysed to obtain the flat band potential by the measurement of a space charge capacitance. It gives a correlation between charge density and electrostatic potential. Since the electrostatic potential cannot be measured directly the most valuable information can be obtained from the capacitance measurement of a space charge layer. Thus the measurement of differential space charge layer capacitance provides a convenient tool, for obtaining the useful informations about both the semiconductor and an electrolyte. For semiconductor electrolyte solar cells, the capacitance observed corresponds to the semiconductor depletion layer, since the capacitances due to Helmholtz and Gouy diffuse layers are assumed negligible due to high ionic concentration of an electrolyte. The capacitance is related to voltage as [ 41, 117 ]:

$$C^{-2} = \frac{2}{q \cdot \epsilon_s \epsilon_0 N_D} \left[ V - V_{fb} - \frac{kT}{q} \right] \quad \dots 5.7$$

where,  $\epsilon_s$  is a dielectric constant of a semiconductor,  $\epsilon_0$  is permittivity of the free space,  $N_D$  is the carrier density and  $V$  is the applied voltage,  $V_{fb}$  is the flat band potential.

The measurement of capacitance - electrode potential vs. ( SCE ) was performed for a cell as explained in chapter III. The capacitance was found to decrease with increased electrode potential. The Mott - Schottky plot is constructed

from these measurements and is shown in fig 5.4. It has been found that the variation of  $C^{-2}$  vs.  $V$  (vs SCE) shows deviation from the straight line behaviour at high applied reverse voltages. The non - linearity is an indicative of the fact that the n-Bi<sub>2</sub>S<sub>3</sub> / electrolyte junction is of graded type [41,67,118]. The departure from an ideal behaviour has been caused by non-uniform d.c. current distribution ( owing to an edge effect, non planar interface, surface roughness etc. ), the presence of both types of impurities, ionic adsorption on the surface of the semiconductor material and partly to the surface states [67,118]. Extrapolation of  $C^{-2}$  vs  $V$  plot to the voltage axis gives the magnitude of the flat band potential,  $V_{fb}$ . The  $V_{fb}$  is of the order of -0.7 V (vs SCE). Since the  $V_{fb}$  is a measure of potential which must be applied to the semiconductor such that the bands remain flat at the interface, the  $V_{fb}$  determines the amount of band bending. The magnitude of  $V_{fb}$  is in close agreement with that reported by Pawar et.al. [261].

C) The current - voltage characteristic in light.

The dynamic I-V curve under 100mW/cm<sup>2</sup> illumination intensity was recorded by means of a variable D.C. power supply, and is shown in fig 5.1 . When a PEC cell is irradiated, the current - voltage characteristic shifts in fourth quadrant, thus, indicating a generator of an electricity which is in accordance with the standard

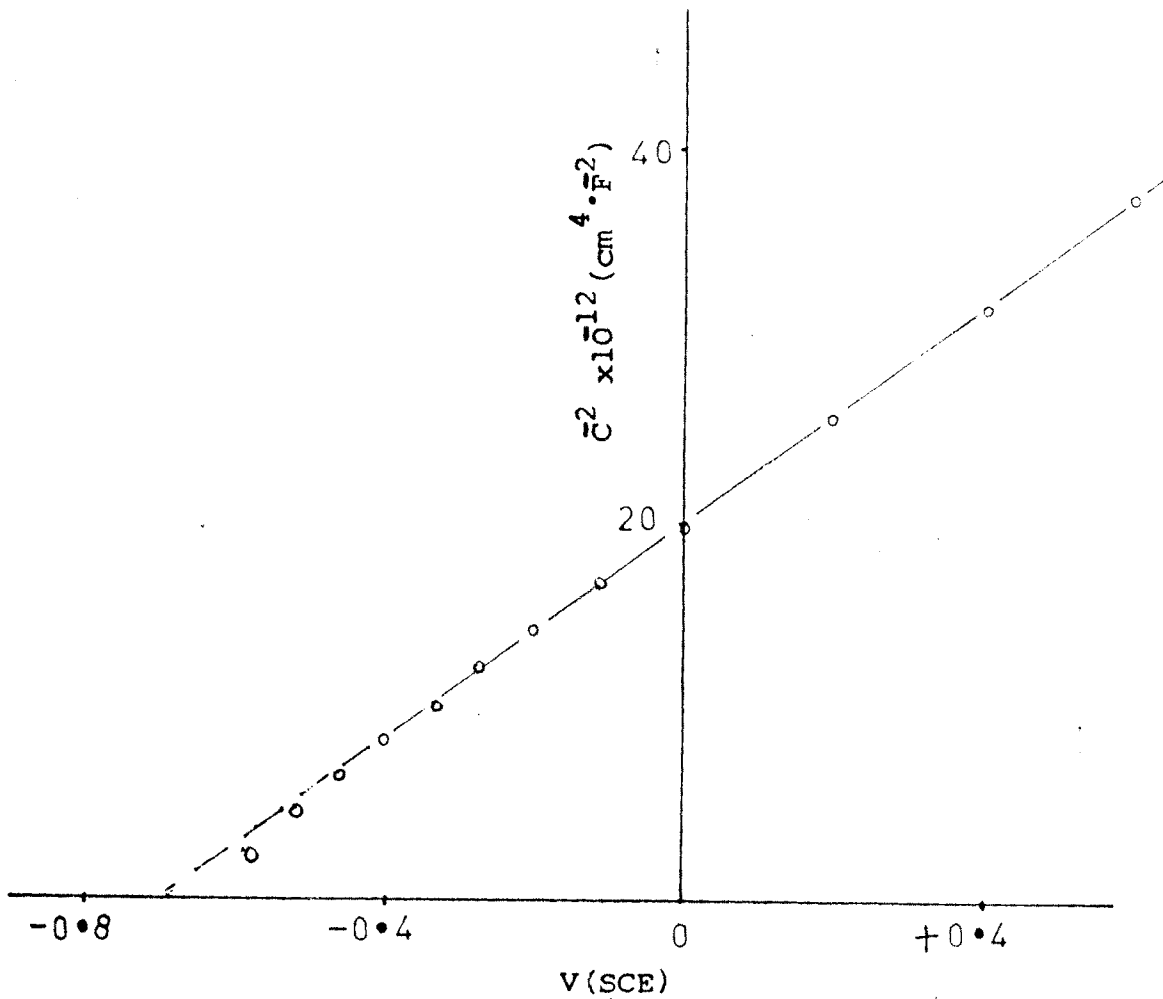


Fig.5.4. Mott-Schottky plot for the PEC cell formed with  $n\text{-Bi}_2\text{S}_3$  photoelectrode.

principles of the PEC cells [119]. It has been found that, under unbiased condition the photoelectrode becomes more and more negative upon illumination showing that the material is n-type [120]. This is in confirmity with the observations on thermoelectric power. The generation of a photovoltage and a photocurrent property of a photoelectrochemical cell can be understood from the equivalent circuit of a cell. The equivalent circuit is shown in fig. 5.5. The photocurrent is represented by a current source. If forward current of a junction is  $I_d$ , the series resistance of a cell is represented by a fixed lumped resistance  $R_s$  which arises from the bulk resistance of a material [41, 83]. The back contact of the cell is considered to be ohmic and an electrolyte offers a negligible resistance to the flow of current. The shunting effect through micro pores and along the edges of a material is shown as  $R_{sh}$  [83].  $R_L$  is the load resistance to the cell and  $V_{oc}$  is the open circuit voltage obtainable from a cell. We consider the Schottky diode equation for the S/E interface and thus the total current of a cell under illumination can be given as [10].

$$I = I_L - I_d - \frac{V_{oc}}{R_{sh}} = I_L - I_0 \left[ \exp\left(\frac{qV}{\eta_j RT} - 1\right) \right] - \frac{V_{oc}}{R_{sh}} \quad \dots 5.8$$

where,  $I_L$  is the photocurrent,  $I_d$  is the dark current,  $I_0$  is the reverse saturation current and  $V$  is the applied voltage. As  $R_{sh}$  for the cell is expected to be very high  $V_{oc} / R_{sh}$  is meaningless and equation (5.8) takes the form as :

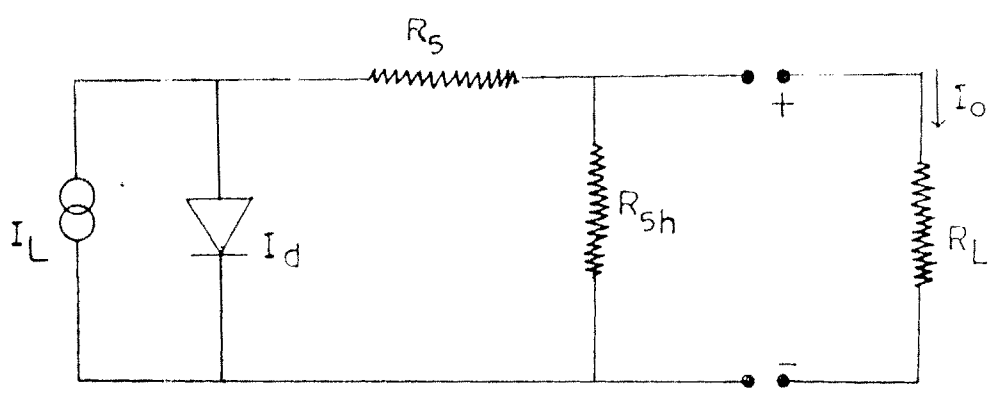


Fig.5.5. The equivalent circuit of a PEC cell.

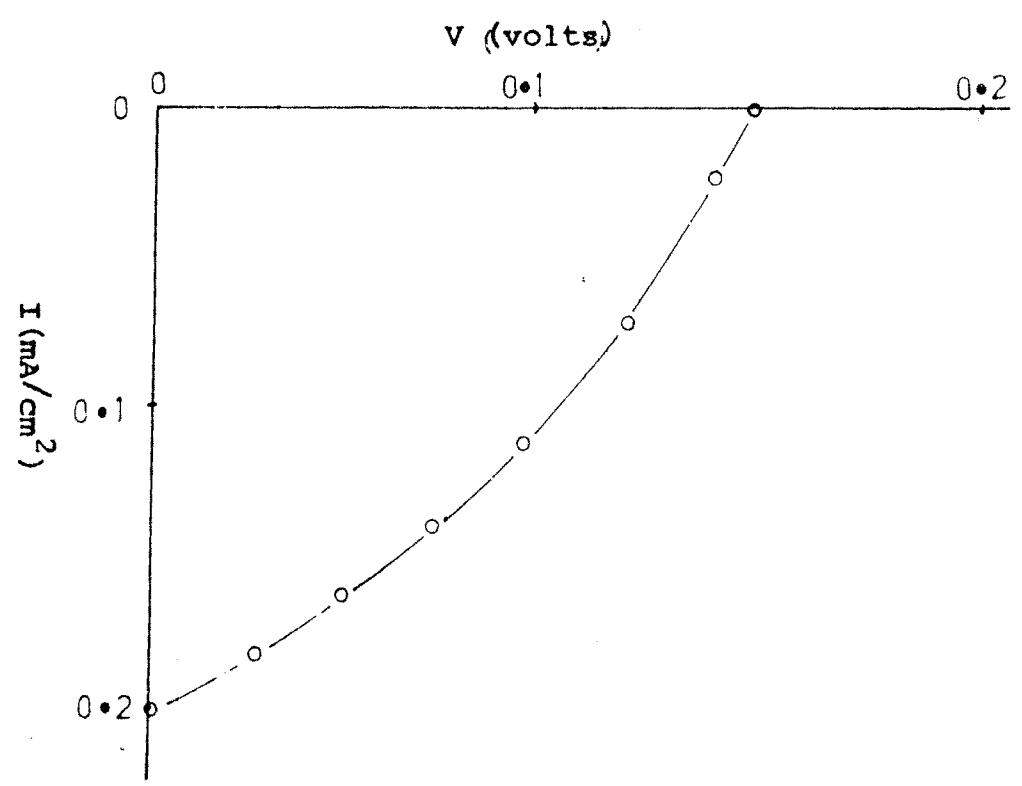


Fig. 5.6 Photovoltaic power output curve.

$$I = I_L - I_0 \left[ \exp\left(\frac{qV}{n_L kT}\right) - 1 \right] \quad \dots 5.9$$

For bias voltages exceeding  $3kT/q$  one can also neglect last term in equation 5.9. Moreover, at open circuit condition  $I_L = I_d$  and  $V = V_{oc}$ , thus rearrangement of equation yields to [10,41] :

$$V_{oc} = \frac{n_L \cdot kT}{q} \ln \cdot \frac{I_{sc}}{I_0} \quad \dots 5.10$$

At short circuit condition  $V_{oc} = 0$  and

$$I = I_L - I_0 = I_{sc} \quad \dots 5.11$$

The I-V characteristic in light is reproduced to obtain power output at an input illumination of  $100 \text{ mW/cm}^2$  (Fig. 5.6). The series resistance  $R_s$  and shunt resistance  $R_{sh}$  have been calculated and are 400 ohms and 1600 ohms respectively. The fill factor  $ff(35.15\%)$ , and energy conversion efficiency  $\eta$  (0.012%), are computed from the power output curve.

### 5.3.2 Optical Properties :

The three major optical features studied for a cell are : photoresponse, spectral response, and speed of response.

#### a) Photoresponse:

The dependence of short circuit current,  $I_{sc}$ , and open circuit voltage,  $V_{oc}$  of a cell have been noted as a function of illumination light level,  $F_L$  as depicted in fig. 5.7 . It is seen that  $I_L$  has a direct bearing on  $F_L$  for low level of excitation and obeys the relation [24] :

$$I = C \cdot F_L \quad \dots 5.12$$

where,  $C$  = constant of proportionality which depends on the fraction of light utilised for the generation of the number of carriers. The photoelectrochemical reactions at the semiconductor - electrolyte interface can be observed if minority carriers are generated by light absorption and finally they can reach the photoelectrode surface during their life time. The net current is therefore, dependent on various competing processes. The externally measurable current therefore, is a difference between the actual photocurrent and the forward current of the majority carriers. If the later is decreased to zero only photocurrent can be observed as :

$$I_{ph} = I - I_{redox} \quad \dots 5.13$$

where,  $I$  = observed total current and  $I_{redox}$  current due to oxidation - reduction with surface states. In the absence of surface recombination and fast rate of electron transfer, the photocurrent increases steeply with  $F_L$  [121].

The variation of  $V_{oc}$  with the  $F_L$ , shows (Fig. 5.7) saturation beyond  $60 \text{ mW/cm}^2$  light level which clearly indicates that  $V_{oc}$  depends upon the extent of band bending and change in the photo-fermiclevel of the photoelectrode [121]. For an ideal photovoltaic device the dependence of  $V_{oc}$  should follow equation (5.10), which defines the movement of fermi level in the bulk with increasing light intensity. Above  $60 \text{ mW/cm}^2$  input intensity the surface states

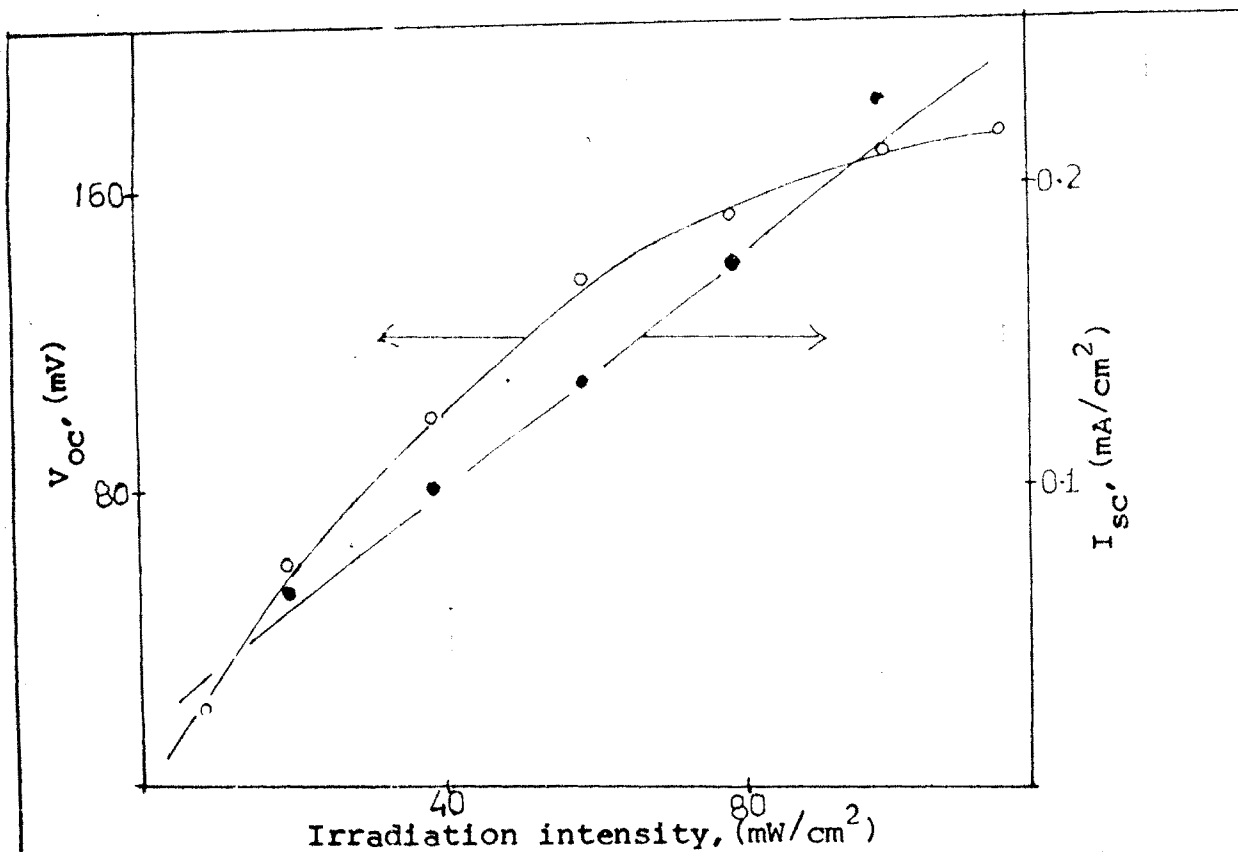


Fig.5.7. Variation of  $V_{OC}$  and  $I_{SC}$  with intensity of illumination. (Intensity measured with a Lutron Lux meter Lx-10)

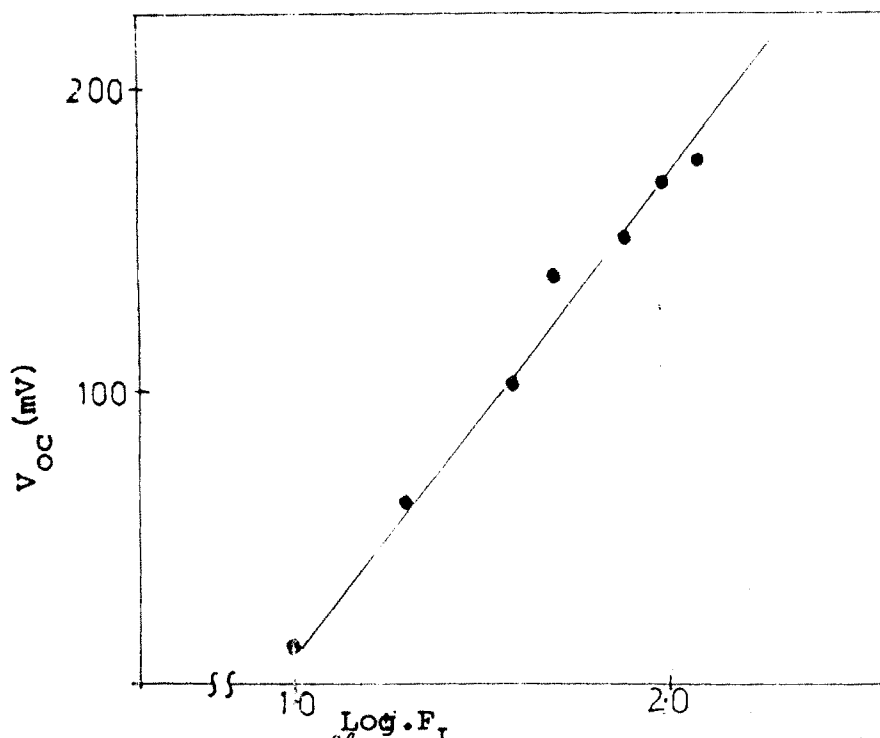


Fig.5.8. Determination of lighted quality factor ( $n_L$ ) of a PEC junction with  $n\text{-Bi}_2\text{S}_3$  as a photoelectrode.

act as recombination centres [121] which cause to saturate the open circuit voltage resulting into low fill factor (ff) and efficiency ( $\eta$ ) [122]. The photoresponse spectra is further analysed to determine the lighted quality factor of an illuminated junction. A plot of  $V_{OC}$  vs.  $\ln.F_L$  is shown in fig.5.8 for  $I_0 \ll I_{sc}$ . The  $n_L$  can be determined from the slope of this plot and is found to be 2.49, slightly smaller than  $n_d$ . This is in accordance with the results reported by Deshmukh et.al [41].

b) Spectral response :

The spectral response is an important technique utilised for the determination of the mode of transition of the semiconductor. There are some other techniques to determine this mode of transition, such as photoconductivity, reflectance, photoemission, intrinsic conductivity, optical absorption and electroreflectance, however these are tedious than that of the spectral response. The response involves the measurement of short circuit current with wavelength. This is shown in fig.5.9. Before the measurement, the dark current of a cell has been nullified by using a potentiometric arrangement as shown in the fig.5.10. The cell was mounted on a photospectrometer and short circuit current was measured for various wavelengths ranging from 400nm to 1000 nm. It is observed from the response that the photocurrent decreased both for shorter as well as longer

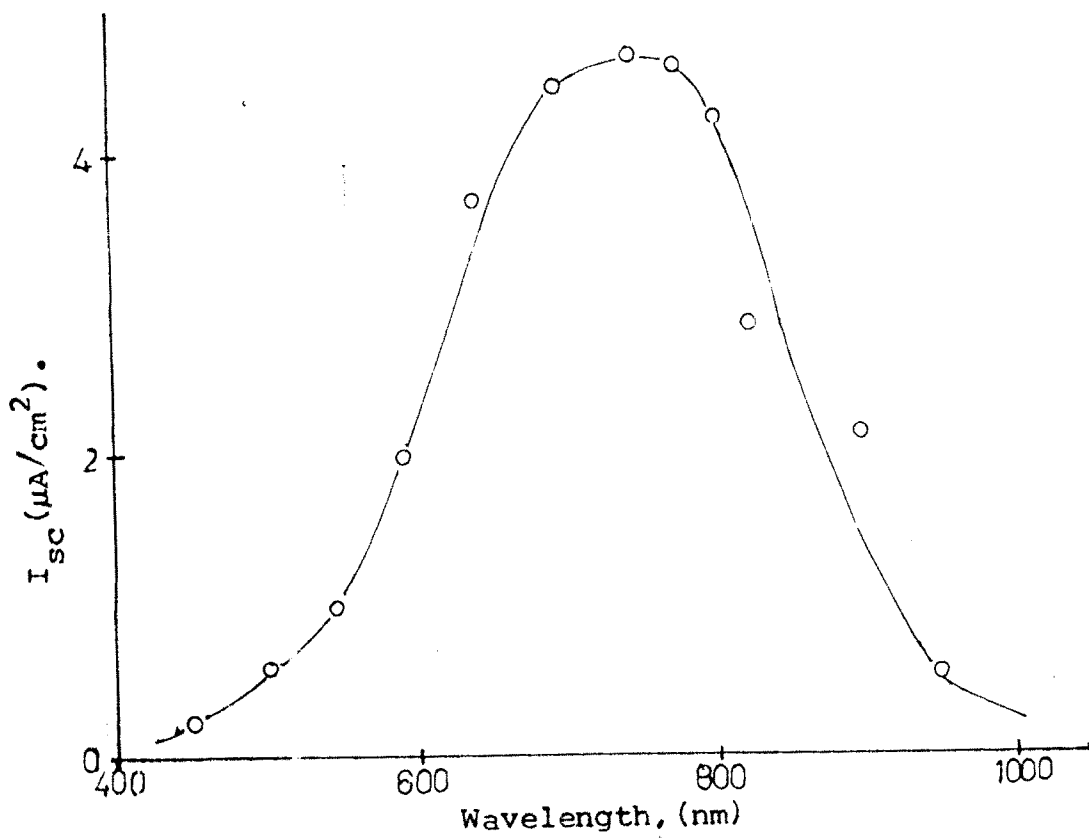


Fig.5.9.Spectral response of n-Bi<sub>2</sub>S<sub>3</sub> based PEC cell.

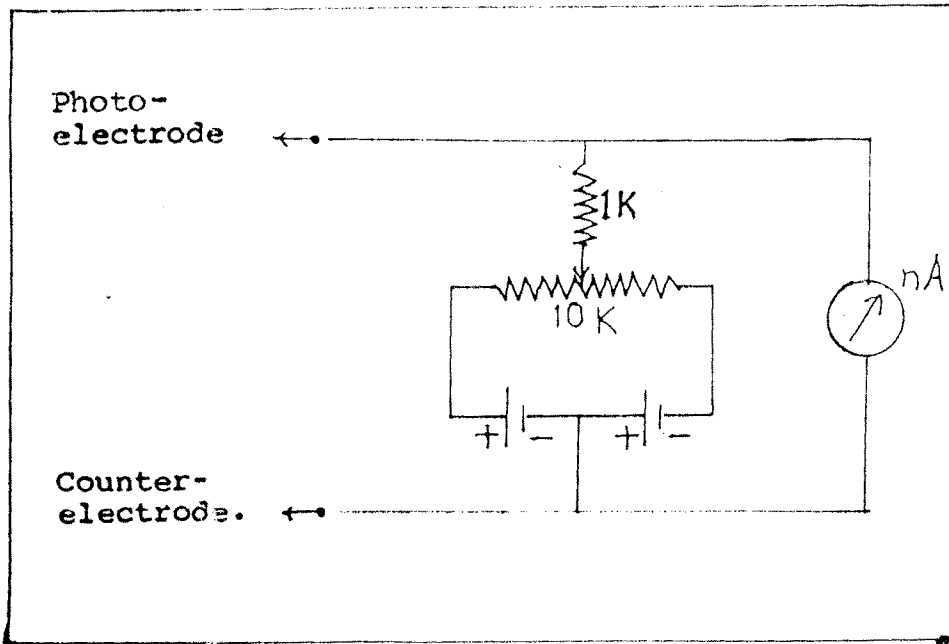


Fig.5.10.An arrangement for nullifying the dark current of a cell while measuring a spectral response.

wavelengths. Photocurrent decay on longer wavelength side is attributed to the non-optimised thickness and transition between defect levels [123]. The decrease in current on shorter wavelength side is due to the absorption of light into an electrolyte and presence of surface recombination centres and to damages or impurities in the bulk very near the surface [123]. Thus spectral response gives a remarkable conclusion regarding the impediment of the hole transfer, across the semiconductor electrolyte interface. The spectral response also gives an information regarding the optimal band gap of a material for an efficient absorption, the theoretical consideration being 1.4 eV. In addition to the optimal band gap it is desirable to use semiconductor with direct electronic transition modes. According to Gartner's model [124] one can analyse the photocurrent density,  $I_{ph}$  of a cell near the absorption edge as:

$$I_{ph} = C \frac{(h\nu - E_{ind})^2}{h\nu} \quad (\text{for indirect mode}) \dots 5.14$$

and

$$I_{ph} = C \frac{(h\nu - E_d)^{1/2}}{h\nu} \quad (\text{for direct mode}) \dots 5.15$$

We can expand  $I_{ph}^2$  of equation (5.15) in the parameter  $h\nu - E_d$  up to a linear term (in this case  $I_{ph}^2$  is linear with  $h\nu$ ) close to  $E_d$  and it vanished at  $h\nu = E_d$ . This helped us to determine the band gap of the material under study. Thus

plotting  $I_{ph}^2$  vs.  $h\nu$  the value of energy gap can be determined. Fig. 5.11 shows the energy gap of n-Bi<sub>2</sub>S<sub>3</sub> to be 1.45 eV.

C) Speed of response :

The speed of response characteristic of a PEC cell is the rise and decay of  $I_{sc}$  and  $V_{oc}$  with time. Time required for  $I_{sc}$  and  $V_{oc}$  to decay to its original value after removal of the light excitation is known as decay time. In the present investigation  $V_{oc}$  decay is studied in order to understand the charge transfer mechanism of an electrolyte. Most of the role of charge transport is played by the ions in an electrolyte.  $V_{oc}$  decay for the cell n-Bi<sub>2</sub>S<sub>3</sub>/1M OH<sup>-</sup> + 1M S<sup>2-</sup>/C is shown in fig.5.12. Relatively fast rise and slow decay is observed at 100 mW/cm<sup>2</sup> light intensity.

The decay of  $V_{oc}$  follows the relation of second order kinetics [24] as:

$$V_{oc}(t) = V_{oc}(0) t^{-b} \quad \dots 5.16$$

where  $V_{oc}(0)$  and  $V_{oc}(t)$  are open circuit voltages at  $t=0$  and at  $t$  seconds and  $b$  is the rate constant. Further slow decay in  $V_{oc}$  is ascribed to the presence of surface states and hence the Fermi level pinning.

In conclusion, a photoelectrochemical cell formed with chemically deposited n - Bi<sub>2</sub>S<sub>3</sub> shows, at this stage, a poor performance relative to cells formed with other materials. The major reason is its high electrical

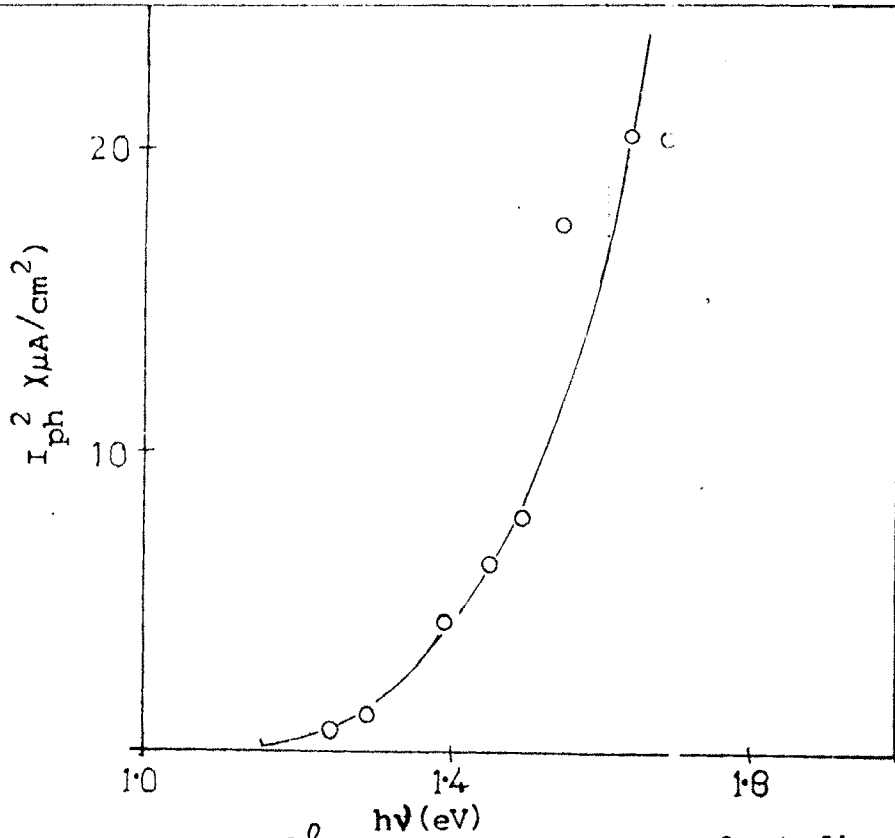


Fig.5.11. Estimation of  $E_g$  bandgap from spectral studies.

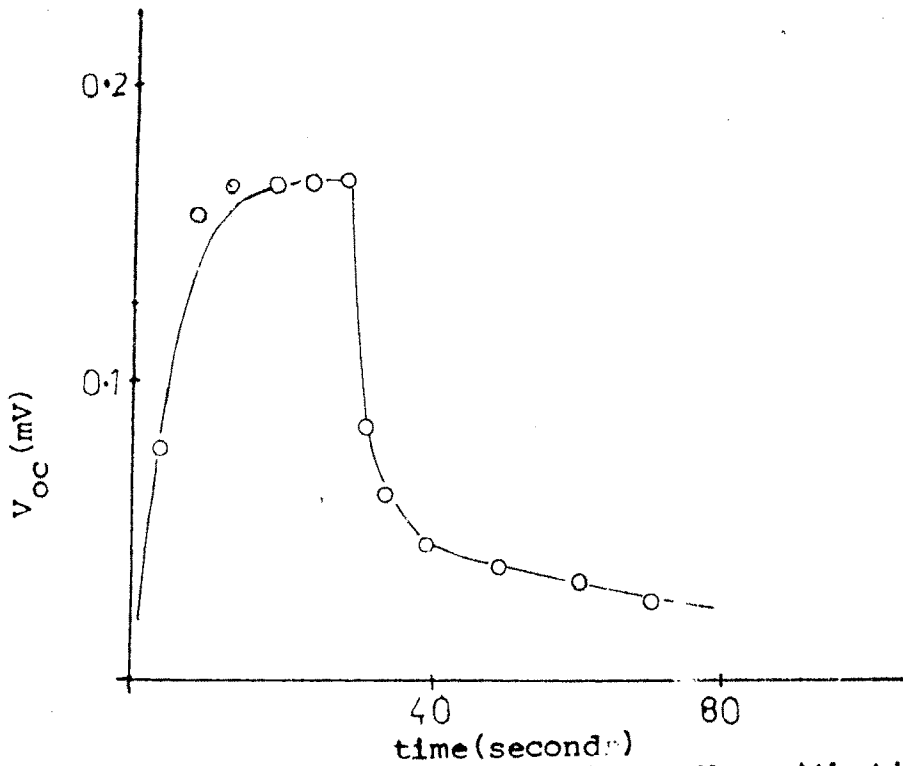


Fig.5.12. Variation of open circuit voltage  $V_{OC}$  with time.

resistivity and should be decreased in order to extract an expected power output. Attempts are now in progress to optimise the material in various views such as Bi : S ratio, dopant concentration , post preparative treatments, thickness of the photoelectrode , series diode type of cell formation etc.